THE JOURNAL OF BIOLOGICAL CHEMISTRY VOL. 282, NO. 16, pp. 11874–11884, April 20, 2007

Role of Phosphatidylinositol 3-Kinases in Chemotaxis in *Dictyostelium*[*]

Received for publication, November 29, 2006, and in revised form, February 5, 2007 Published, JBC Papers in Press, March 1, 2007, DOI 10.1074/jbc.M610984200

Kosuke Takeda[‡], Atsuo T. Sasaki[§1], Hyunjung Ha[§2], Hyun-A Seung[§2], and Richard A. Firtel[‡3]

From the [‡]Section of Cell and Developmental Biology, Division of Biological Sciences and [§]Center for Molecular Genetics, University of California, San Diego, La Jolla, California 92093-0380

Experiments in several cell types revealed that local accumulation of phosphatidylinositol 3,4,5-triphosphate mediates the ability of cells to migrate during gradient sensing. We took a systematic approach to characterize the functions of the six putative Class I phosphatidylinositol 3-kinases (PI3K1–6) in *Dictyostelium* by creating a series of gene knockouts. These studies revealed that PI3K1–PI3K3 are the major PI3Ks for chemoattractant-mediated phosphatidylinositol 3,4,5-triphosphate production. We studied chemotaxis of the *pi3k1/2/3* triple knock-out strain (*pi3k1/2/3* null cells) to cAMP under two distinct experimental conditions, an exponential gradient emitted from a micropipette and a shallow, linear gradient in a Dunn chamber, using four cAMP concentrations ranging over a factor of 10,000. Under all conditions tested *pi3k1/2/3* null cells moved slower and had less polarity than wild-type cells. *pi3k1/2/3* null cells moved toward a chemoattractant emitted by a micropipette, although persistence was lower than that of wild-type or *pi3k1/2* null cells. In shallow linear gradients, *pi3k1/2* null cells had greater directionality defects, especially at lower chemoattractant concentrations. Our studies suggest that although PI3K is not essential for directional movement under some chemoattractant conditions, it is a key component of the directional sensing pathway and plays a critical role in linear chemoattractant gradients, especially at low chemoattractant concentrations. The relative importance of PI3K in chemotaxis is also dependent on the developmental stage of the cells. Our data suggest that the output of other signaling pathways suffices to mediate directional sensing when cells perceive a strong signal, but PI3K signaling is crucial for detecting weaker signals.

Chemotaxis, or directed cell movement in response to a small molecule ligand, is a basic process of many cell types and is essential for a variety of physiological processes including inflammatory responses, innate immunity, cellular morphogenesis, and metastasis of cancer cells (1–4). Cells respond to a directional signal by extending the pseudopod or lamellipod in the direction of the chemoattractant gradient through the localized polymerization of F-actin. Coordinated with this response is retraction of the posterior of the cell via a myosin II-mediated pathway. Studies over the past few years have elucidated many of the molecular mechanisms controlling this response. One of the major findings is that key aspects of the regulatory mechanisms that control chemotaxis are similar in neutrophils and *Dictyostelium* cells, suggesting they are highly conserved through evolution.

Class I PI3-kinases (PI3Ks)[4] have been implicated in controlling chemotaxis in *Dictyostelium*, neutrophils, and macrophages. Initial studies in *Dictyostelium* followed by those in neutrophils and fibroblasts demonstrated that PI3K is locally activated at the leading edge of chemotaxing cells (5–8). These studies employed reporters in which GFP was fused to the PH domain of CRAC or Akt/PKB. These PH domains preferentially bind to the Class I PI3K products PI(3,4,5)P_3 and PI(3,4)P_2. Real-time, dynamic PH domain localization studies demonstrated that the PH domain-containing proteins are cytosolic and rapidly localize to the site of the plasma membrane closest to the chemoattractant source. This localization is dependent on PI3K, as determined by sensitivity to the PI3K inhibitor LY294002 and its absence in *pi3k* null cells. Null mutants of some *Dictyostelium* proteins with PIP_3-responsive PH domains exhibit defects in cell movement and chemotaxis, suggesting that PI3K is involved in chemotaxis (7, 9–11). In *Dictyostelium*, the two previously studied PI3Ks, PI3K1 and PI3K2, have Ras binding domains, which are required for chemoattractant-stimulated PI3K activation (12). Ras is rapidly activated at the leading edge (peaking at 3–4 s) (13). Cells in which Ras function is abrogated have difficulty polarizing and, once they do, are unable to effectively sense the direction of the chemoattractant gradient and move randomly. The initial activation of Ras and PI3K is independent of F-actin polymerization. However, F-actin polymerization is essential for amplifying the signal and stabilizing the leading edge in neutrophils and *Dictyostelium* (13, 14). In *Dictyostelium*, F-actin recruits additional PI3K to the newly forming leading edge, enhancing the PIP_3 response and downstream effector function (13, 15). Cells with decreased

* This work was supported by United States Public Health Service grants (to R. A. F.). The costs of publication of this article were defrayed in part by the payment of page charges. This article must therefore be hereby marked "*advertisement*" in accordance with 18 U.S.C. Section 1734 solely to indicate this fact.

The nucleotide sequence(s) reported in this paper has been submitted to the GenBank™/EBI Data Bank with accession number(s) XM_642316, XM_635069, and XM_630307.

[1] Present address: Lewis Cantley Laboratory, Harvard Medical School, New Research Building Room 152, 77 Ave. Louis Pasteur, Boston, MA 02115.

[2] Present address: Dept. of Biochemistry, School of Life Sciences, Chungbuk National University, Cheongju 361-762, Korea.

[3] To whom correspondence should be addressed: Natural Sciences Bldg. Rm. 6316, University of California, San Diego, 9500 Gilman Dr., La Jolla, CA 92093-0380. Tel.: 858-534-2788; Fax: 858-822-5900; E-mail: rafirtel@ucsd.edu.

[4] The abbreviations used are: PI3K, phosphatidylinositol 3-kinase; GFP, green fluorescent protein; PH, pleckstrin homology; PI(3,4,5)P_3, phosphatidylinositol 3,4,5-triphosphate; PI(3,4)P_2, phosphatidylinositol 3,4-diphosphate; PIP_3, phosphatidylinositol 1,4,5-trisphosphate; RBD, Ras binding domain; CRAC, cytosolic regulator of adenylyl cyclase.

PI3K activity exhibit a decrease in the second peak of RacB activation and F-actin polymerization, which has been linked to pseudopod extension.

Dictyostelium cells lacking two of the Class I PI3Ks (*pi3k1/2* null cells) show defects in directionality under some experimental conditions, although these cells can still move toward the chemoattractant source (10). *pi3k1/2* null cells developed for 5 h have reduced polarity and produce lateral pseudopodia; however, under other developmental conditions this strain behaves indistinguishably from wild-type cells (16). Neutrophils lacking PI3Kγ or in which PI3Kγ has been inhibited by drugs that show specificity for this Class I PI3K isoform exhibit decreased directionality of cell movement (14, 17–19). Macrophages in which PI3Kδ function is impaired exhibit decreased cell polarity (20). Studies using LY294002 have provided contradictory results in a variety of cell types (21). In *Dictyostelium*, brief treatment with LY294002 renders cells unable to effectively sense the direction of the chemoattractant source; however, after 5 or more min, these cells become polarized and move up a strong chemoattractant gradient (10, 16). The mammalian RacGEF DOCK180, which can promote cell migration, is dependent on $PI(3,4,5)P_3$ for signaling; a related member of this RacGEF subfamily, DOCK2, is required for lymphocyte chemotaxis (22–26). Carcinoma cells employ a phospholipase C/cofilin-mediated directional signaling pathway while incorporating PI3K as an important component for the secondary F-actin response (27, 28).

Evidence from studies in carcinoma and *Dictyostelium* cells has implicated PI3K in the control of F-actin polymerization (28, 29). In response to a global (uniform) stimulation of cells in suspension, *Dictyostelium* and mammalian cells show a biphasic F-actin polymerization response. There is an initial rapid and transient peak (~5 s in *Dictyostelium*) followed by a rapid decrease in F-actin polymerization and a subsequent slower rise producing a broad peak at ~30–60 s. The second peak has been linked to the extension of the pseudopod and is dependent on PI3K in both *Dictyostelium* and carcinoma cells (28, 29). *pi3k1/2* null cells (developed for 5 h) and LY294002-treated wild-type cells have reduced RacB activation that has been linked to F-actin polymerization in the *Dictyostelium* strain KAx-3. *pten* null cells, which exhibit elevated and temporally extended $PI(3/4)P_2$/$PI(3,4,5)P_3$ accumulation, have elevated levels of the second peak of RacB activation and F-actin polymerization (30).

To further elucidate and define the roles of PI3K in chemotaxis, we have undertaken a more detailed analysis of the role of PI3Ks in *Dictyostelium*. Examination of the completed *Dictyostelium* genome has identified six Class I PI3Ks (this manuscript and Ref. 31). By creating single, double, and some triple knock-out mutations, we have genetically titrated the level of functional PI3K in *Dictyostelium* cells. We used these cells to study chemotaxis in response to a point source of chemoattractant (chemoattractant emitted from a micropipette), which produces an exponential gradient (very steep near the micropipette and flat far from the micropipette), and cells responding to a linear gradient of chemoattractant produced using a two-well chemotaxis chamber (Dunn chamber). Our studies indicate that as one decreases the level of functional PI3K in cells, the chemotaxis phenotypes become more severe. A triple PI3K1/2/3 knock-out strain that can respond to a steep chemoattractant gradient is unable to effectively chemotax to a shallow, linear gradient, exhibiting defects in directionality of cell movement. We found that the defects are also dependent on the concentration of the chemoattractant and the developmental stage of *Dictyostelium* cells. We suggest PI3K is a component of a complex cellular compass whose integrated function is to control the directional response of the cell.

EXPERIMENTAL PROCEDURES

Cell Culture and Development—The *Dictyostelium* strain KAx-3 was grown in axenic HL5 medium and transformed by electroporation. For gene disruption we selected cells in the presence of blasticidin or hygromycin.

Gene Identification and Sequence Analysis—The dictyBase (dictybase.org) was screened for other putative PI3Ks using the kinase domain of PI3K1, PI3K2, or PI3K3 (GenBank™ accession numbers U23476, U23477, and XM_638728, respectively). We identified three additional putative Class I PI3Ks, DDB0216567, DDB0204875, and DDB0189237. We named DDB0216567 as PI3K4, DDB0204875 as PI3K5, and DDB0189237 as PI3K6 (GenBank™ accession numbers XM_642316, XM_635069, and XM_630307, respectively), BLAST, Smart, and SCAN programs were used to analyze the obtained sequences. Alignments were made using ClustalW.

Gene Disruption—Gene inactivation was obtained by replacing part of the gene with the Bsr or Hyg cassette. The cassette was inserted into the BamHI site (nucleotide 3435 from ATG on genomic DNA) of PI3K3, the BglII site (nucleotide 3096) of PI3K4, the EcoRV site (nucleotide 3811) of PI3K5, and the BglII site (nucleotide 4093) of PI3K6. Potential knockouts were screened by PCR and confirmed by Southern blot analyses.

Chemotaxis and Image Acquisition—The analyses of chemotaxis toward cAMP were done as described previously (10, 13) and analyzed with the DIAS program (32). To obtain developmentally competent cells capable of responding to cAMP as a chemoattractant, log-phase vegetative cells were washed once, resuspended at a density 5×10^6 cells/ml, and pulsed with cAMP for 5–7 h (time of pulsing is indicated in each figure legend) at 6-min intervals. We added LY294002 to a final concentration of 50 μM 20 min before real-time recording of chemotaxis toward the micropipette emitting the chemoattractant.

Biochemical Assay—Akt/PKB activity was measured as described previously (7).

RESULTS

Extended Treatment of Cells with the Chemoattractant cAMP Partially Rescues pi3k1/2 Null Cell Chemotaxis Defects—The chemotactic responsiveness of *Dictyostelium* cells to the chemoattractant cAMP is a developmentally regulated process in which the expression of both the major cAMP chemoattractant receptor (cAR1) and the coupled Gα subunit (Gα2) is very low during vegetative growth and is induced to high levels during the early stages of development before aggregation (33, 34). In addition to acting as a chemoattractant, cAMP induces this developmental program, which controls the aggregation of cells to form

A

Strain name	Wild-type	*pi3k1* null	*pi3k2* null	*pi3k3* null	*pi3k4* null	*pi3k5* null	*pi3k6* null
PKB activity after 10 sec (WT=100%)	100	60	29	74	102	103	100
Speed (μm/min)	12.3±1.4	7.7±0.9	6.3±1.0	7.3 ±1.4	11.9±0.2	12.7±1.0	12.7±2.0
Directionality	0.91±0.01	0.63±0.06	0.56±0.10	0.77±0.14	0.81±0.15	0.73±0.05	0.72±0.03
Roundness (%)	66.9±5.7	41.9±2.8	51.1±2.8	49.3±2.2	61.2±7.9	51.6±2.6	44.9±1.9

Strain name	*pi3k1/2* null	*pi3k2/3* null	*pi3k2/4* null	*pi3k2/5* null	*pi3k2/6* null	*pi3k1/2/3*null
PKB activity after 10 sec (WT=100%)	16	N.D	N.D	N.D	N.D	6
Speed (μm/min)	6.0±0.8	4.9±0.5	7.3±1.9	8.4±1.6	6.5±0.5	6.2±0.5
Directionality	0.41±0.17	0.47±0.31	0.65±0.14	0.81±0.11	0.66±0.06	0.30±0.20
Roundness (%)	73.8±12.0	64.1±1.4	61.2±5.1	51.9±4.2	56.3±12.8	63.7±16.4

B

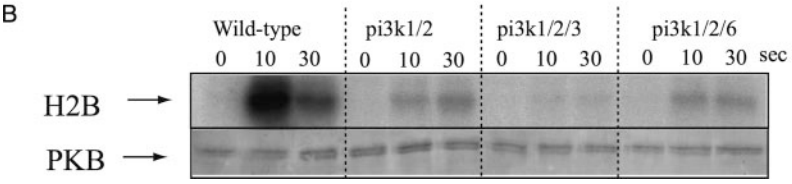

FIGURE 1. **Analysis the properties of PI3K strains.** *A*, DIAS analysis of chemotaxis. Relative Akt/PKB activation was normalized to Akt/PKB activation of wild-type cells, with the level of Akt/PKB activity at 10 s after stimulation taken as 100%. A wild-type control experiment was also performed with each mutant strain analysis and internally compared. Cells were pulsed with 30 nM cAMP for 5 h at 6-min intervals. DIAS computer analysis was performed from digital time-lapse video differential interference contrast microscopy movies of the listed strain chemotaxing to cAMP. A 40× or 20× objective was used. Cells were plated onto the coverslip in the chemotaxis chamber and let stand for 20–30 min before insertion of the micropipette. Cells were recorded for 30 min. Analysis was done on images starting 15 min after insertion of the micropipette. The speed of movement of the centroid is indicated. Change in direction (in degrees) is a relative measure of the number and frequency of turns the cells make. The parameter measures the change (in degrees) in the position of new pseudopodia (leading edges) relative to the position of the cell centroid. A higher number indicates more turns and less efficient chemotaxis. Roundness is an indication of the polarity of the cells. A larger number indicates the cells are rounder (less polarized). Directionality is a measure of how straight the cells move. Cells moving in a straight line have a directionality of 1.0. It is calculated as the distance moved over the linear distance between the start and the finish. *B*, chemoattractant-mediated activation (kinase assay) of Akt/PKB in wild-type and *pi3k1/2*, *pi3k1/2/3*, and *pi3k1/2/6* null cells (H2B as a substrate). *Upper lanes* show the kinase assay. *Lower lanes* show a Western blot of Akt/PKB protein in the immunoprecipitate. Akt/PKB activity was measured as described previously (7). Experiments were repeated three times. Wild-type cells are always assayed in parallel with the mutant strains, and the relative levels of Akt/PKB activity are internally compared within each experiment.

a multicellular organism, and regulates a signal relay system to activate adenylyl cyclase and, thus, transiently increase its own synthesis. This developmental pathway can be induced in cell suspension by pulsing cells with exogenous cAMP to mimic the endogenous signal produced by cells during normal development (35). This cell suspension system is generally employed to obtain "developmentally competent" cells able to respond to cAMP for use in chemotaxis assays.

Wild-type cells pulsed with cAMP for 5 h (using the protocol described previously (10)) are fully competent to respond to cAMP, maximally induce known signaling pathways required for chemotaxis (F-actin polymerization, myosin II assembly, and Akt/PKB activation), and maximally induce cAMP-mediated early gene expression (10). These cells become highly polarized when placed in a chemoattractant gradient and chemotax with a speed equal to that of cells pulsed for a longer time (7 h; data not shown). When a micropipette containing a chemoattractant is placed on the lateral side of a 5-h pulsed, polarized, chemotaxing cell, the cell changes direction predominantly by producing a new pseudopod at the side of the cell closest to the micropipette (10). Such cells produce a localized activation of Ras and PI3K, as observed through the localization of GFP-Ras binding domain fusion and GFP fusion of a PH domain-containing protein (CRAC, Akt/PKB, PhdA) at the side of the membrane closest to the micropipette (13). This site becomes the site of localized F-actin polymerization and the formation of a new pseudopod. Thus, these cells are highly plastic in that they are able to rapidly change direction through the activation of "leading edge responses" at the side of the cell closest to the micropipette and through the formation of the new pseudopod at this site.

When wild-type cells are pulsed for 7 h, they can become highly polarized even in the absence of an exogenous chemoattractant signal, presumably due to the high endogenous production and secretion of cAMP, as this does not happen with adenylyl cyclase null cells (36, 37). Wild-type cells pulsed for 7 h readily form head-to-tail streams of cells that prevent effective analysis of single cells. Seven-hour-pulsed cells also tend to turn by changing the direction of the leading edge when the position of the micropipette is moved (unless it is very close to the cells) rather than inducing a new leading edge at the side of the cell, indicating these cells have a very stable leading edge.

We previous characterized the chemotactic behavior of *pi3k1/2* null cells pulsed for 5 h, which exhibit wild-type levels of pulse-induced gene expression, using a micropipette filled with 150 μM cAMP to produce a chemoattractant gradient (10). As in previous reports, 5-h-pulsed *pi3k1/2 null* cells are more rounded and move more slowly and with poorer directionality than wild-type cells (summarized in Fig. 1*A*, data not shown). Because of the controversy on the chemotaxis phenotypes of *pi3k1/2* null cells in the literature (16), we investigated the effect of extending pulsing (development) on the *pi3k1/2* null cell phenotypes. Seven-hour-pulsed *pi3k1/2* null cells do not readily form streams, presumably because of defects in the activation of adenylyl cyclase (38), which allows one to examine the effect of increased pulsing on the chemotaxis behavior of these cells. As shown in Fig. 2, *pi3k1/2* null cells pulsed for 7 h move as well as wild-type cells with respect to speed and directionality, consistent with recently published results (16). Thus, we find that longer pulsing rescues the *pi3k1/2* null cell chemotaxis

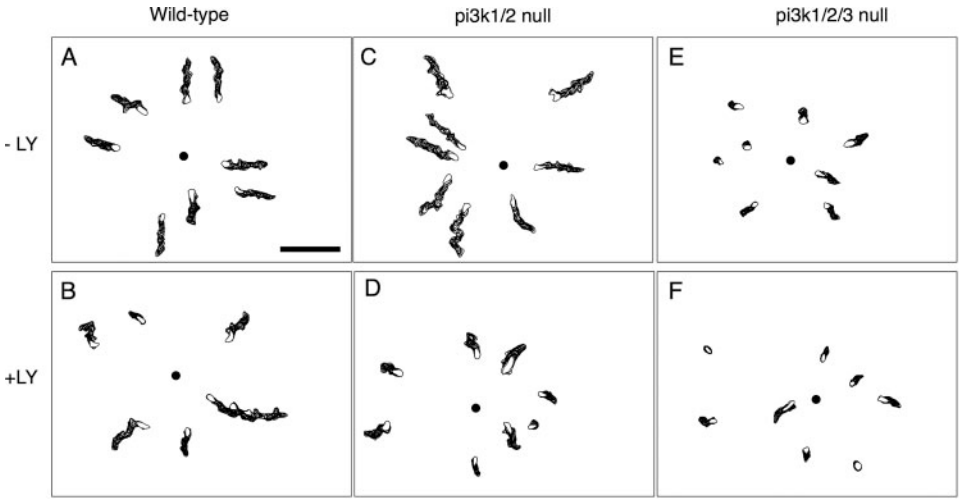

G

Strain name	Wild-type	Wild-type	pi3k1/2 null	pi3k1/2 null	pi3k1/2/3 null	pi3k1/2/3 null
LY (50 μM)	-	+	-	+	-	+
Speed (μm/min)	11.6+/- 1.6	9.1+/-2.7	14.7+/-1.6	6.9+/-1.1	5.1+/-1.3	4.7+/-1.2
Directionality	0.87+/-0.05	0.76+/-0.13	0.84+/-0.05	0.53+/-0.14	0.52+/-0.20	0.37+/-0.19
Direction change (deg.)	15.3+/-3.4	24.8+/-13.2	17.1+/-2.9	42.9+/-7.6	44.4+/-11.5	58.1+/-15.5
Roundness (%)	76.2+/-6.1	73.6+/-4.4	67.7+/-9.1	79.3.1+/-6.1	83.5+/-9.3	79.3+/-10.6

FIGURE 2. **Chemotactic behavior of wild-type, *pi3k1/2*, and *pi3k1/2/3* null cells with and without LY294002 treatment.** *A–F*, time-lapse recording of wild-type, *pi3k1/2*, and *pi3k1/2/3* null cells. A *closed circle* indicates the position of a micropipette containing 150 μM cAMP. Wild-type cells were pulsed for 6 h, and *pi3k1/2* and *pi3k1/2/3* null cells were pulsed for 7 h (see the legend to Fig. 1 for details). For treatment with LY294002, cells were incubated with 50 μM LY294002 for 20 min before inserting the micropipette. The drug was also present during the time of the recording. The depictions of the pathways and shapes of chemotaxing cells were obtained using DIAS computer software (32). The overlapping images are taken at 6-s intervals. The *scale bar* is 100 μm. *G*, analysis of chemotaxis using DIAS software. See the legend to Fig. 1 for details.

defects. Cyclic AMP-stimulated Akt/PKB activation, which is reduced to ~16% that of wild-type cells, is unaffected by increased pulsing (Fig. 1*A* and *B*; data not shown; Ref. 10), suggesting that the behavioral difference between 5- and 7-h-pulsed cells is not due to an increase in PI3K activity. These findings suggest that the difference in chemotaxis behavior between 5- and 7-h-pulsed cells may be due to one or more PI3K-independent pathways involved in controlling directional movement and that this difference may be associated with different developmental timing.

Identification of Six Phosphatidylinositol 3-Kinases in Dictyostelium—We had previously identified three Class I PI3Ks (PI3K1, 2, 3) in *Dictyostelium* (39). Three additional genes were revealed in the recently completed *Dictyostelium* genome sequence project (Fig. 3, *A* and *B*; Ref. 31). PI3K1–5 have a long N-terminal domain, a Ras binding domain (RBD), a C2-domain, a kinase accessory domain, and a kinase catalytic domain, similar to metazoan Class I PI3Ks. Analysis of the kinase domains indicates that PI3K1 and PI3K2 are most closely related to human Class Ia and Ib PI3Ks, whereas the PI3K6 kinase domain is most closely related to that of the Class III PI3K VPS34.

PI3K6 lacks an RBD but has a PH domain in approximately the same location as the RBD in PI3K1–5 (Fig. 3*A*). The PI3K6 PH domain shows sequence divergence from PH domains known to preferentially bind $PI(3,4)P_2$/$PI(3,4,5)P_3$. Some PH domains bind lipids and a number of PH domain-containing proteins, including those that preferentially bind $PI(3,4)P_2$ and $PI(3,4,5)P_3$, localize to the cortex in response to chemoattractant stimulation. We created a GFP-PI3K6 PH domain fusion and examined its subcellular localization in unstimulated and stimulated cells. The reporter remained cytosolic in all assays and did not bind $PI(3,4)P_2$ or $PI(3,4,5)P_3$ in lipid dot blot assays (data not shown).

We demonstrated previously that there is a low level of PI3K1 and PI3K2 at the cell cortex, which dramatically increases in response to chemoattractant stimulation (13). In response to global stimulation, this translocation is transient and is dependent on F-actin polymerization but not dependent on the RBD or the C-terminal C2 or catalytic domains. To examine whether this dynamic subcellular localization is general for the *Dictyostelium* Class I PI3Ks, we examined PI3K3, another member of this family that contains a RBD, and PI3K6, which has a PH domain and no RBD. We found that PI3K3 exhibits a subcellular localization profile similar to those of PI3K1 and PI3K2; GFP-PI3K3 is predominantly cytosolic and rapidly translocates to the cortex upon chemoattractant stimulation (data not shown). Furthermore, PI3K3 localizes to the leading edge in chemotaxing cells (Fig. 4*A*). In contrast, PI3K6 shows a significant cortical localization in unstimulated cells. Unexpectedly, PI3K6 becomes localized to the posterior of polarized, chemotaxing cells (Fig. 4*B*), similar to the localization of p21-activated kinase A and adenylyl cyclase A, the adenylyl cyclase that produces cAMP during aggregation (38).

PI3K3 Is a Third PI3K Implicated in PIP_3 Production by cAMP Stimulation—We examined the effect of the PI3K inhibitor LY294002 on chemotaxis. Within 1 min of addition, drug-treated cells round up and are unresponsive to chemoattractant. Although wild-type cells respond and start to produce pseudopodia within 15–20 s after inserting the micropipette, there is a 10–15-min delay before 7-h-pulsed wild-type cells treated with the drug start to polarize and move toward the micropipette, although they do so with an increased directional change (decreased persistence or linearity of movement) compared with wild-type cells (Fig. 2). The speed of movement is also decreased relative to wild-type cells. We then studied the chemotaxis behavior of *pi3k1/2* null cells in the presence of the PI3K inhibitor LY294002. As shown in Fig. 2, LY294002 treatment results in a significant decrease in speed and an increase in directional change as described by Loovers *et al.* (16). This finding suggests that other PI3Ks and/or non-PI3K, LY294002-sensitive pathways, such as TORC2 (40), may play a role in cell movement.

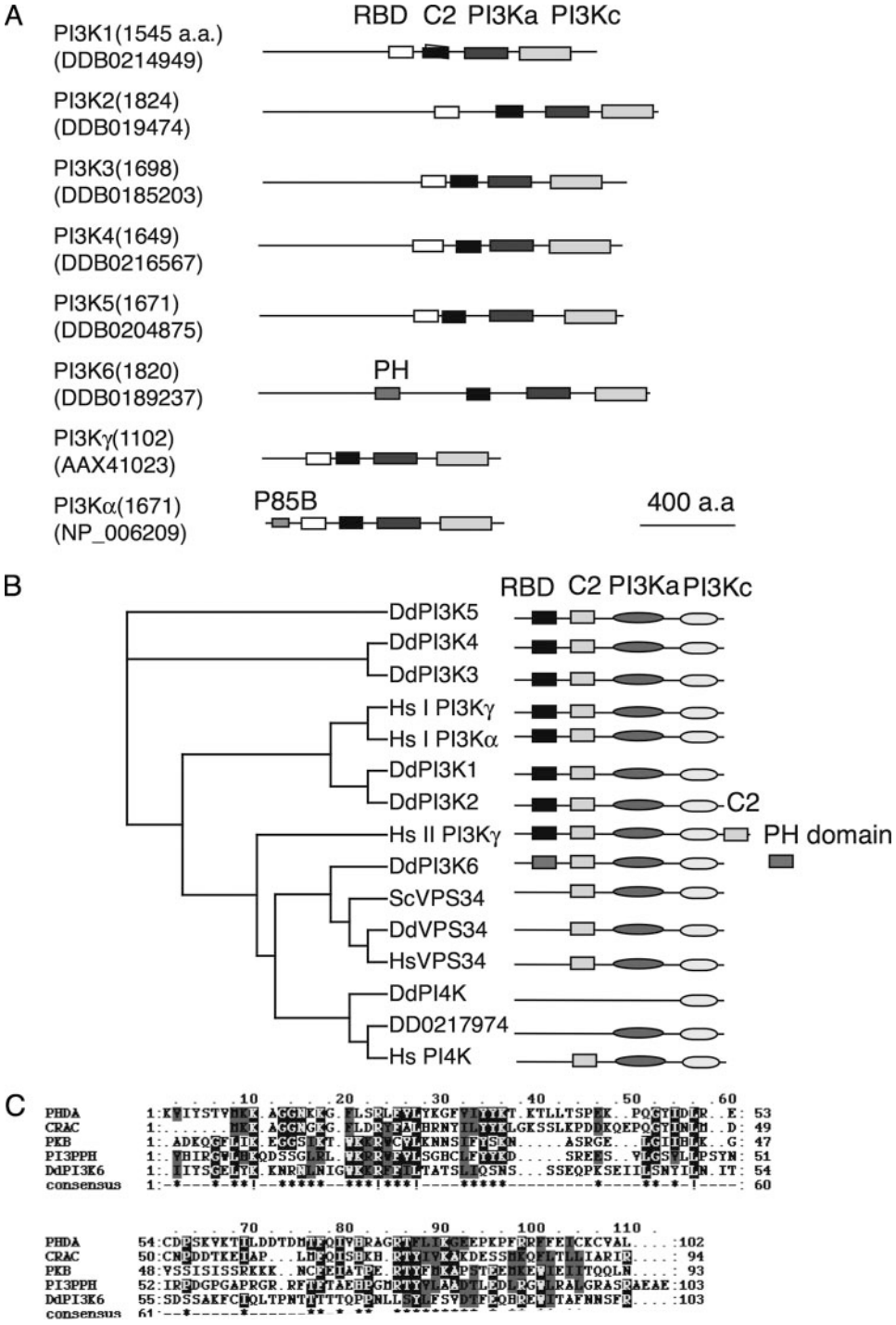

FIGURE 3. **The PI3K family in *Dictyostelium*.** *A*, schematic diagram of PI3K domain structures of the *Dictyostelium discoideum* PI 3-kinases DdPI3K1–6 and the human PI3Ks. The proteins PI3K1, PI3K2, and PI3K3 are encoded by *pikA*, *pikB*, and *pikC*, respectively. We name the genes encoding PI3K4, PI3K5, and PI3K6 *pikF*, *pikG*, and *pikH*, respectively. *pikE* encodes the *Dictyostelium* VPS34, and *pikF* encodes PI4K. We name the gene encoding a second PI4K, DDB0217974, *pikI*. *B*, cluster analysis of the kinase domain of PI3- or PI4-kinase from *Dictyostelium* and other eukaryotes. *C*, sequence comparison of the PH domain of PI3K6 with other PH domains. Genes: developmental protein *PhdA*, *D. discoideum* AAC29444; *PKBA*, *D. discoideum* U15210; *CRAC*, *D. discoideum* AAA61782; phosphoinositol 3-phosphate-binding protein-1 (*PI3PPH*), *Homo sapiens* AAG01896; *DdPI3K6*, *D. discoideum*, XM_630307.

To identify which PI3Ks might be involved in Akt/PKB activation and chemotaxis, we created knock-out strains for all 6 PI3Ks by homologous recombination and investigated the effect of gene inactivation on Akt/PKB activation and chemotaxis by determining the response of the cells to cAMP emitted from a micropipette. Single gene disruptions of PI3K1, -2, and -3 result in reduced Akt/PKB activation (Fig. 1, *A* and *B*). Because we have shown that the chemotaxis defects of *pi3k1/2* null cells are greater when cells are pulsed for 5 h than for 7 h, we used 5-h-pulsed cells to examine potential chemotaxis defects in the initial screen of the *pi3k* null strains to maximally visualize possible defects. As described previously and summarized in Fig. 1*A*, *pi3k1* and *pi3k2* null strains have reduced Akt/PKB activation and reduced chemotactic parameters (Fig. 1*A*; Ref. 10). In addition, *pi3k3* null cells exhibit decreased responsiveness to cAMP in these assays. *pi3k4*, *pi3k5*, and *pi3k6* null strains have no observable phenotypes. The single gene knockouts grow normally in axenic medium and on bacterial lawns (data not shown). When the cells are plated for development, no defects in timing or morphology are observed.

To better assess the relative input of the different PI3Ks in regulating chemoattractant-mediated responses, we created a series of double PI3K gene knockouts *pi3k1/3*, *pi3k2/3*, *pi3k2/4*, *pi3k2/5*, *pi3k1/6*, and *pi3k2/6* null strains. The majority of these were examined for chemotaxis defects (assayed after 5 h of pulsing). None of the strains displayed defects stronger than those of *pi3k1/2* null cells, whereas *pi3k2/3* null cells exhibited a similar defect (Fig. 1*A*; data not shown). We also created a *pi3k1/2/6* knock-out. This strain behaved indistinguishably from *pi3k1/2* null cells in our chemotaxis and Akt/PKB assays (Fig. 1, *A* and *B*; data not shown). Our chemotaxis and quantitative Akt/PKB activation analyses, thus, indicate that PI3K1, -2, and -3 have major input into chemoattractant-mediated Class I PI3K function in *Dictyostelium* in response to chemoattractant stimulation (Fig. 1*B*; data not shown). Overexpression of PI3K6 does not restore chemoattractant-mediated Akt/PKB activity when expressed in *pi3k1/2* null cells (data not shown). This result plus the homology of the PI3K6 kinase

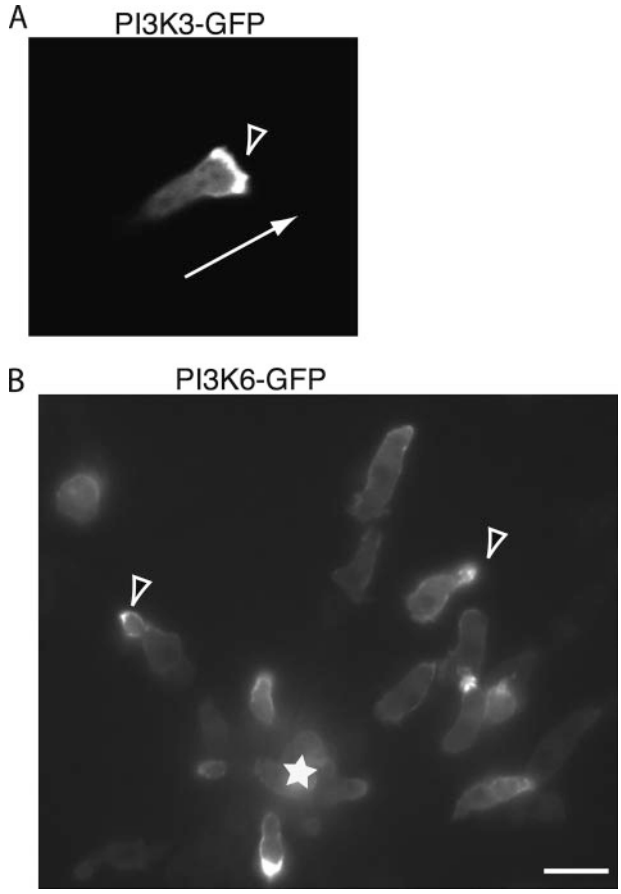

FIGURE 4. **Localization of PI3K6-GFP during chemotaxis.** Fluorescent images of PI3K3-GFP (*A*) and PI3K6-GFP (*B*) expressed in wild-type cells exposed to chemoattractant gradient. The *asterisk* indicates the position of the micropipette (*B*). The *open arrows* show the location of PI3K3-GFP (*A*) and PI3K6-GFP. The *arrow* in *A* points toward the chemoattractant source. The *scale bar* is 20 μm.

domain to that of VPS34 and PI3K6 posterior localization suggest it may function in pathways very different from those regulated by PI3K1–5. Because PI3K1, -2, and -3 are the major isoforms contributing to Class I PI3K activity during chemotaxis, we created a *pi3k1/2/3* triple null strain. Akt/PKB activation in the *pi3k1/2/3* triple null strain was ~6% that of wild-type (Fig. 1*B*), lower than that of the *pi3k1/2* double knock-out, which is already severely reduced compared with that of wild-type cells (Fig. 1*A* and *B*; Ref. 10). As expected, no chemoattractant-stimulated PH domain translocation (using GFP-CRAC or GFP-PKB) was observed in response to chemoattractant stimulation (data not shown). Although *pi3k1/2* null cells exhibit mild developmental defects as previously described, *pi3k1/2/3* null cells do not aggregate (Fig. 5*A*). We also find that *pi3k1/2/3* null cells have a fairly severe growth defect (Fig. 5*B*). *pi3k1/2* null cells also show a growth defect, as reported previously (39), but not as severe as that of the *pi3k1/2/3* null strain.

Chemotaxis of pi3k1/2/3 Null Cells—We investigated chemotaxis in *pi3k1/2/3* null cells after 7 h of cAMP pulsing using our micropipette assay under standard conditions (Eppendorf Femtotip containing 150 μM cAMP, no applied pressure; Ref. 10). DIAS computer analysis (Fig. 2) indicates that *pi3k1/2/3* null cells move significantly slower than wild-type cells (wild-type cells are pulsed for 6 h; longer pulsing results in a high level of cell streaming). The persistence of chemotaxis (directionality or linearity of movement, see legend to Fig. 1) is also reduced, although the majority of these cells move toward the micropipette. Thus, *pi3k1/2/3* cells null cells move up the chemoattractant gradient but do so less efficiently than wild-type cells. Treatment of these cells with LY294002 results in a small increase in directional change. As with other strains treated with this drug, cell movement does not commence until ~15 min after the cells are placed in the gradient. We also noticed that the cells that do move are those closest to the micropipette, where the cAMP gradient is the steepest and the concentration the highest. Pulsing *pi3k1/2/3* null cells for 8 or 9 h does not "rescue" the *pi3k1/2/3* chemotaxis defects (data not shown).

To examine if the reduced chemotactic speed of the *pi3k1/2/3* null cells is due to a decrease in the intrinsic rate of cell motility or due to reduced chemoattractant-induced cell movement (chemokinesis), we quantitated the cell movement of 7-h-pulsed *pi3k1/2/3* null cells. As shown in Fig. 6, *pi3k1/2* null cells have a speed of motility similar to that wild-type cells, whereas that of *pi3k1/2/3* null cells is significantly reduced.[5] The *pi3k1/2/3* null cells exhibit both a decrease in cell movement and a decrease in chemokinesis. Both *pi3k1/2* and *pi3k1/2/3* null cells have reduced persistence compared with wild-type cells (the paths of cells are shorter before changes of direction).

Characterization of Cell Migration in Shallow Gradients and to Low Concentrations of Chemoattractant—To examine the effect of the concentration of the chemoattractant on chemotaxis behavior, we assayed the chemotaxis of wild-type cells and *pi3k1/2* and *pi3k1/2/3* null cells using a micropipette filled with three different cAMP concentrations (150, 15, and 1.5 μM cAMP; Fig. 2 shows analysis for 150 μM cAMP; data not shown). With 150 μM cAMP, >80% of cells in the field of all strains positively moved toward the micropipette. At 1.5 μM cAMP, only 45% of wild-type cells and 25% of *pi3k1/2/3* null cells (data not shown) positively moved toward the micropipette. Furthermore, the cells that moved were predominantly those closest to the micropipette where the concentration of chemoattractant was highest.

Concentration gradients established from a point source (micropipette) by diffusion are exponential and are, thus, very nonlinear near the chemoattractant source, in the region normally used for chemoattractant analysis. Such assay conditions were, therefore, not useful in examining the effect of the chemoattractant gradient on directional movement. In visually examining movies using the micropipette assay system, we found that the chemotaxis behavior of cells was affected by their distance from the micropipette. We, therefore, used a Dunn chamber to generate a more shallow, linear gradient. Dunn chambers have two wells and a connecting bridge. The chemoattractant and/or buffer is placed in each well, and a concentration gradient rapidly forms across the bridge. The cells are placed on the bridge. Movement of the cells on the bridge can be readily viewed and recorded. We examined the migration of wild-type cells in this system over a 10,000-fold difference in cAMP concentrations (1 μM, 100 nM, 10 nM, 1 nM, or 100

[5] A. T. Sasaki, C. Janetopoulos, K. Takeda, S. Lee, P. G. Charest, L. W. Sundheimer, R. Meili, P. N. Devreotes, and R. A. Firtel, submitted for publication.

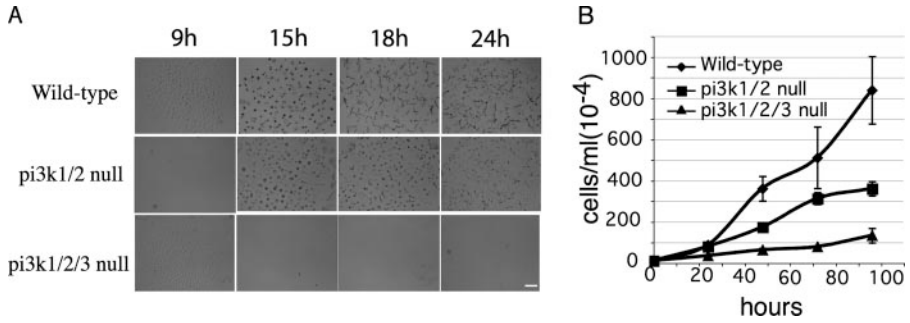

FIGURE 5. **The phenotype of *pi3k1/2* and *pi3k1/2/3* null cells.** *A*, development of wild-type, *pi3k1/2* null, and *pi3k1/2/3* null cells plated on non-nutrient agar. The *scale bar* is 1 mm. *B*, curves show growth of shaking (suspension) cultures of wild-type, *pi3k1/2* null, and *pi3k1/2/3* null cells in HL5 medium.

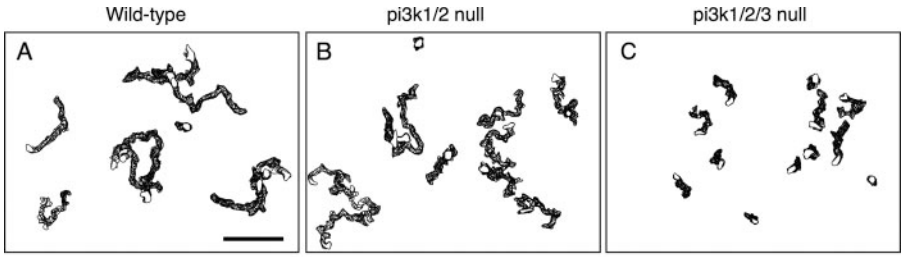

D

Strain name	Wild-type	pi3k1/2 null	pi3k1/2/3 null
Speed (μm/min)	11.7 +/- 4.0	12.3 +/- 5.9	5.8 +/- 1.7
Directionality	0.51 +/- 0.19	0.36 +/- 0.17	0.35 +/- 0.18
Direction change (deg)	37.2 +/- 13.1	32.5 +/- 19.2	51.4 +/- 14.2
Roundness (%)	72.6 +/- 11.0	63.1 +/- 8.2	78.2 +/- 9.3

FIGURE 6. **Basic cell motility of *pi3k1/2* and *pi3k1/2/3* null cells.** *A–C*, time-lapse recording of wild-type, *pi3k1/2* null, and *pi3k1/2/3* null cells as described in the legend of Fig. 1. *D*, analysis of chemotaxis using DIAS software (32). See the legend to Fig. 1 for details. Wild-type cells were pulsed for 6 h; *pi3k1/2* null and *pi3k1/2/3* null cells were pulsed for 7 h.

pM cAMP in one well and buffer in the other well). In all assays, we individually (manually) traced and analyzed (using the DIAS computer program) ~70–75 different cells for each strain under each experimental condition. Images were captured every 6 s over 20 min. Cells were randomly chosen from several movies recorded on different days for each strain and condition.

Our analyses revealed that wild-type cells start to move toward the cAMP source within 5 min (approximately the time it takes for a "stable" gradient to form) and continue to move for more than 30 min. In gradients of 0–1 μM and 0–100 nM cAMP (1 μM and 100 nM in one well, respectively, and buffer in the other well), ~90% of wild-type cells moved positively toward the cAMP source in 20 min (see Fig. 8*A*; data for 1 μM are indistinguishable from those for 100 nM and are not shown; positive movement is defined here as the final position of the cell being closer to the chemoattractant source than its initial position at the start of the analysis, irrespective of the path taken). Using 1 nM cAMP, ~62% of wild-type cells moved toward the cAMP source, and with 100 pM cAMP, wild-type cells showed random movement, similar to when buffer was placed in both wells (~50% of the cells moved toward one well, and ~50% moved toward the other well or parallel to the well).

We tested speed, directionality, and cell shape of 7-h-pulsed *pi3k1/2* and *pi3k1/2/3* null cells. *pi3k1/2* null cells showed directionality similar to that of wild-type cells (Figs. 7*C* and 8*A*). *pi3k1/2/3* null cells exhibited a defect in overall upward directionality ("upward directionality" is defined as movement toward the well with chemoattractant in contrast to directionality/persistence, which measures the ratio of the total distance to the linear distance from start to finish; during random movement, by definition, 50% of the cells move toward the well with chemoattractant). At 100 and 10 nM, the percent of positive *pi3k1/2/3* null cells dropped from ~90% (for wild-type cells) to 73%. Computer (DIAS) analysis indicated that *pi3k1/2* cells moved slightly slower than wild-type cells and with decreased upward directionality and persistence (Fig. 7*C*). The cell shape of *pi3k1/2* cells was comparable with that of wild-type cells. However, *pi3k1/2/3* null cell speed and persistence were significantly lower than those of wild-type cells.

To better understand a possible role of PI3K in the directionality of movement, we plotted and displayed the movement of cells using multiple approaches. Figs. 7*A* and 8*B* show tracings of randomly chosen cells for 100 and 10 nM cAMP. These cells are a subset of the 70–75 cells analyzed. As can be seen, the persistence of movement is visibly reduced in the *pi3k1/2* and *pi3k1/2/3* null strains. In Fig. 8*B*, the initial position of the cells is set at 0, and the relative movement is plotted. Cells moving linearly perpendicular to the horizontal plane (*vertical axis*) would have a directionality or persistence of 1.0. This plot shows that *pi3k* null strains have a reduced directionality, with *pi3k1/2/3* null cells showing a stronger defect than *pi3k1/2* null cells. The paths of cells of both strains took multiple turns and were, thus, not very linear, indicating that these strains had defects in maintaining the directionality of their movement up the gradient. The defect was significantly greater with *pi3k1/2/3* null cells. Some of the *pi3k1/2/3* null cells did not move up the chemoattractant gradient.

Fig. 8*B* presents all of the analyzed cells plotted on polar coordinates, displaying their relative end position, which is a function of speed, directionality, and straightness of the path (the scale is ½ for *pi3k1/2/3* null cells; the data were plotted in this way because the null cells move significantly slower than the other strains). The figure illustrates that the vast majority of the wild-type cells move directionally toward the well containing either 100 nM or 10 nM cAMP (experiments using 1 μM show a plot similar to that of 100 nM cAMP; data not shown). The movement of cells in a 0–1 nM gradient revealed little directionality, and cells in a 0–100 pM gradient moved almost randomly (compared with random movement: 0–0 M gradient, both wells having buffer). *pi3k1/2* null cells showed increased

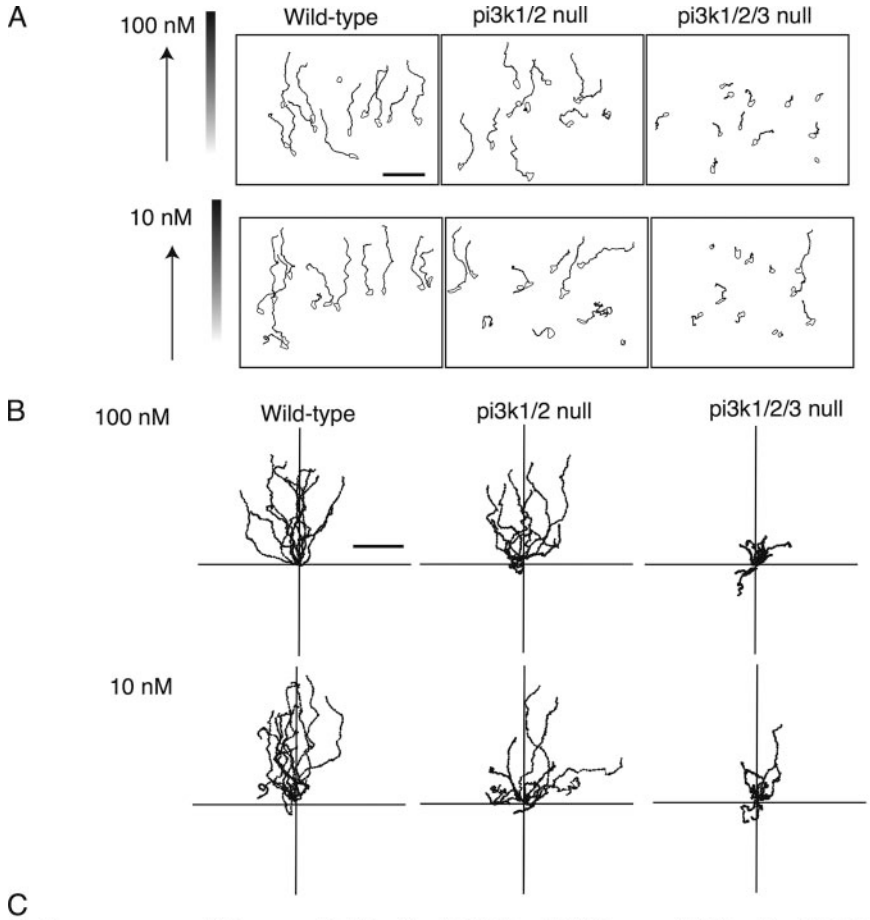

C

Strain name	wild-type	pi3k1//2 null	pi3k1/2/3 null	Wild-type	pi3k1/2 null	pi3k1/2/3 null
cAMP	100 nM	100 nM	100 nM	10 nM	10 nM	10 nM
Speed (μm/min)	13.6+/-3.7	11.6+/-3.9	5.2+/-1.5	15.7+/-3.3	11.2+/-4.6	6.5+/-2.5
Directionality	0.71+/-0.22	0.51+/-0.28	0.39+/-0.14	0.68+/-1.6	0.48+/-0.24	0.30+/-0.21
Upward directionality	0.66+/-0.22	0.45+/-0.29	0.18+/-0.27	0.66+/-0.17	0.29+/-0.31	0.18+/-0.29
Roundness (%)	70.8+/-8.2	69.6+/-11.5	84.7+/-9.8	68.7+/-4.3	68.3+/-11.1	73.2+/-12.4

FIGURE 7. **Migration traces obtained in a Dunn chamber in the presence of shallow cAMP gradients.** *A*, time-lapse recording of wild-type, *pi3k1/2* null, and *pi3k1/2/3* null cells. Images of chemotaxing cells obtained using DIAS computer software. The overlapping images are taken at 6-s intervals. The *scale bar* is 100 mm. *B*, trajectories of cells migrating toward cAMP in Dunn chemotaxis chamber. Trajectories were tracked with DIAS software (32). The *scale bar* is 100 mm. *C*, analysis of chemotaxis using DIAS software. This figure plots the angle between the start and end point of the cell relative to the chemoattractant gradient. Cells in which the end point (relative to the start point) is on a line up the gradient would be plotted as zero (0), no divergence. Cells that lie between −90 and 90 (180°) are cells in which the general direction of movement is up the gradient. The greater the angle, the poorer the ability to sense the direction of the gradient. Cells with an angle of −90 or 90 move perpendicular to the gradient. Cell paths with an angle between −90 and −180 and 90 and 180 move away from the chemoattractant source. These measurements refer to Fig. 1. Wild-type cells were pulsed for 6 h, and *pi3k1/2* and *pi3k1/2/3* null cells were pulsed for 7 h. Upward directionality refers to the relative movement toward the chemoattractant gradient. "Directionality" or persistence as defined by DIAS is the linearity of the movement (distance from the start to the end point divided by the total distance moved).

scatter (less directionality, although the majority of cells in 0–100 nM and 0–10 nM gradients were positive), and *pi3k1/2/3* null cells had an even greater increase in scatter. We plot this analysis as a bar graph that indicates the relative angle of the final position of the cell from its starting position with 0° being linear movement toward the chemoattractant. Cells that have a final position that is perpendicular to the gradient would have an angle of −90° or +90° (Fig. 8*C*; see the legend to Fig. 8 for a further description). Wild-type cells in a 0–100 nM gradient show a sharp distribution that centers around 0°. The spread of the distribution is increased in a 0–10 nM gradient. The distribution spread is greater for *pi3k1/2* null cells and further increased for *pi3k1/2/3* null cells. For both *pi3k* null strains, as with wild-type cells, the spread is greater in a 0–10 than in a 0–100 nM gradient.

When *pi3k1/2/3* null cells were observed for an extended time, after 40–45 min, the speed and persistence of movement up the chemoattractant gradient increased (Fig. 9). The speed increased significantly, but it was still only ~55% that of wild-type cells. Similarly, we found that LY294002-treated wild-type cells did not move or polarize during the first ~15 min in the gradient but then became polarized and moved directionally (there was no change in speed of either wild-type or *pi3k1/2* null cells with time). This delay in responsiveness was also observed by Loovers *et al.* (16), although their observed delay was shorter. We suggest that during this initial period, PI3K-independent pathways are amplified at the leading edge, and these pathways then mediate PI3K-independent chemotaxis (see "Discussion").

DISCUSSION

Many studies have indicated an important role for PI3K in chemotaxis (see the Introduction). The rapid localization of a number of PIP_3-responsive, PH domain-containing proteins to the site on the plasma membrane closest to the chemoattractant source implied that localized PI3K activation was an important part of the directional sensing machinery (see the Introduction). In addition, the expression of a uniformed localized PI3K (myr-PI3K) and deletion of PTEN resulted in adventitious sites of PIP_3 accumulation and pseudopod formation around the perimeter of the cell and an increase in chemoattractant-mediated F-actin polymerization (12, 41). Some studies revealed that disruption or inhibition of PI3K caused decreased chemotaxis efficiency; however, the majority of these studies indicated that PI3K-deficient cells could move directly but with decreased efficacy. Another recent study concluded that PI3K was important for cell polarization but not directional sensing in *Dictyostelium* (16). In this manuscript, we show that PI3K is an important component of directional sensing, although it is not essential under certain conditions (high chemoattractant concentrations and steep gradients). We demonstrate that one possible explanation for the difference between previous studies and this more recent study is the

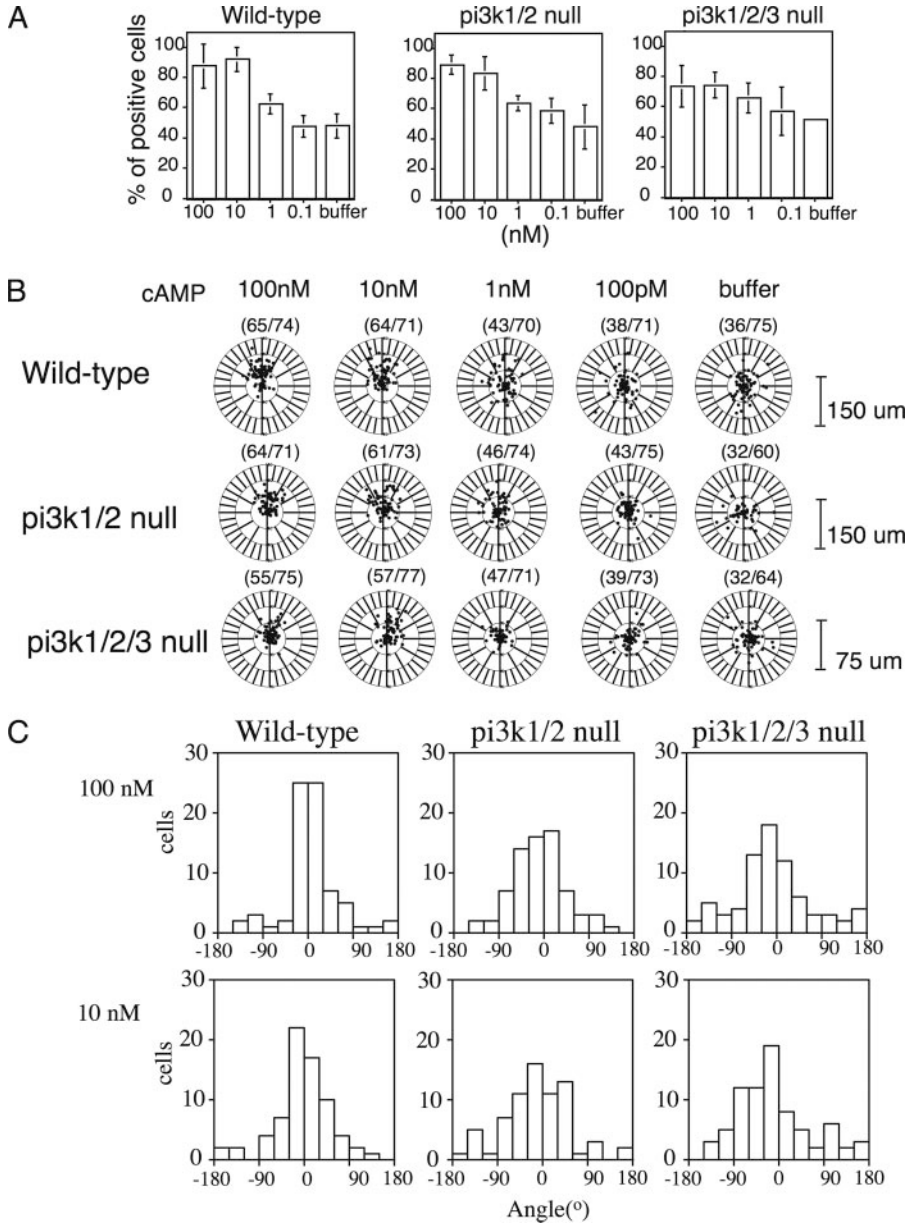

FIGURE 8. **Directional migration of *pi3k* null cells in a cAMP gradient.** *A*, the directed migration of wild-type, *pi3k1/2* null, and *pi3k1/2/3* null cells was assayed in Dunn chemotaxis chamber. The gradient employed was 100 pM to 100 nM cAMP. Chemotactic response to various concentrations of cAMP was compared between wild-type cells, *pi3k1/2* null cells, and *pi3k1/2/3* null cells in Dunn chemotaxis chambers. The results are expressed as the percentage of positively moving cells (mean ± the S.D. of three separate experiments). *B*, the final location relative to the initial position is compared between wild-type, *pi3k1/2* null, and *pi3k1/2/3* null cells. The *cross-marks* indicate the origin. The *numbers* indicate the number of cells that moved positively (toward the source) and the total number of cells analyzed. *C*, the data are presented as a histogram in which the final position of the cell is plotted as an angle relative to its starting position. The number of cells within each 30° increment is given. Cells that move directly to the chemoattractant gradient would have an angle of 0°. Cells which have a final position that is perpendicular to the gradient would have an angle of −90° or +90°. Wild-type cells were pulsed for 6 h, and *pi3k1/2* and *pi3k1/2/3* null cells were pulsed for 7 h.

developmental time of the cells (10, 16). We note that the difference is not simply due to 5-h-pulsed cells being insufficiently competent; there are differences between 5- and 7-h-pulsed cells. One difference is that 5-h cells are more plastic than 7-h cells in responding to directional changes. We suggest that there is more than one directional sensing pathway, and PI3K is a component of this machinery. Cells pulsed for 7 h can compensate for the loss of PI3K better than 5-h cells with the dependence on PI3K being a function of the concentration and steepness of the chemoattractant gradient. We note that *Dictyostelium* has a *bona fide* Akt/PKB that is PI3K-dependent and a related kinase (PKBR1) that lacks a PH domain, is myristoylated, and is PI3K-independent. Genetically, the two genes are interchangeable (7, 9). Akt/PKB is expressed early in development and aggregation and is then degraded, whereas PKBR1 is expressed early, and the level of expression increases during late aggregation. The difference in the relative role of the PI3K pathway in 5- and 7-h cells may be due in part to a difference in the relative contribution of Akt/PKB and PKBR1 activities in 5- and 7-h cells, respectively.

To better understand the possible role for PI3K in chemotaxis, we undertook a genetic approach to titrate the activity of Class I PI3K by deleting various members of this family. We found that 3 of the 5 Class I PI3Ks with a canonical structure detectably contribute to chemoattractant-stimulated Akt/PKB activity. We investigated the chemotactic properties of two multiple gene knock-out strains in further detail; *pi3k1/2* null cells, a strain that had been previously analyzed (10, 16), and *pi3k1/2/3* null cells. Both of these strains moved with only a small decrease in directionality to an exponential gradient of chemoattractant produced by diffusion from a micropipette at the highest concentration of chemoattractant tested. A major difference between the strains was that the *pi3k1/2/3* null cells exhibited a reduced speed of movement, as is also the case for random cell movement.[5] This suggests that PI3K also plays an important role in mediating the speed of cell movement of *Dictyostelium* cells, consistent with the finding that the second peaks of F-actin polymerization and RacB activation are greatly reduced or suppressed in *pi3k1/2* null cells (29, 30). When the concentration of cAMP in the micropipette was reduced, there was a reduction in the persistence of cell movement for the *pi3k* null strains, although cells still moved to the micropipette. This reduction was greater for *pi3k1/2/3* null cells.

We also found that cells further away from the micropipette, where the gradient was shallower, exhibited greater defects.

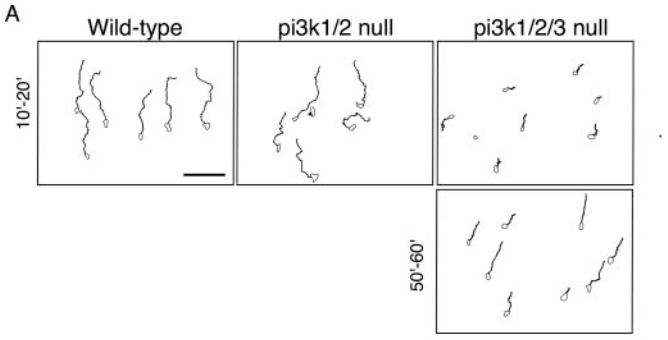

B

Strain name	.Wild-type	pi3k1/2null	pi3k1/2/3 null	pi3k1/2/3 null
Time (min)	10-20	10-20	10-20	50-60
Speed (μ m/min)	15.8 +/- 2.0	13.5 +/- 3.1	5.3 +/- 1.1	8.4 +/- 1.2
Directionality	0.80 +/- 0.03	0.54 +/- 0.28	0.421+/- 0.1	0.73 +/- 0.01
Upward Directionality	0.78 +/- 0.03	0.49 +/- 0.29	0.18 +/- 0.32	0.67 +/- 0.09
Direction change (deg)	14.2 +/- 0.3	25.2 +/- 8.6	52.5 +/- 10.5	28.65 +/- 6.3
Roundness (%)	71.0 +/- 5.1	63.8 +/- 6.0	86.6 +/- 2.1	79.1 +/- 5.1

FIGURE 9. **Effect of time on the chemotaxis of *pi3k1/2/3* null cells in a chemoattractant gradient.** *A*, time-lapse recording of wild-type, *pi3k1/2* null, and *pi3k1/2/3* null cells as described in the legend of Fig. 1. *B*, analysis of chemotaxis using DIAS software (see the legend to Fig. 1). Wild-type cells were pulsed for 6 h; *pi3k1/2* null and *pi3k1/2/3* null cells were pulsed for 7 h.

Our analysis of cells in a Dunn chamber, in which the gradients should be linear over the times tested, revealed a profound difference in the behavior of chemotaxing cells. As the level of PI3K was reduced, the severity of the defects increased. Although the majority of the cells displayed positive movement (the end position of the cell was closer to the chemoattractant source), the straightness of the pathway and the angle of the path decreased. This decrease was more severe at lower concentrations of chemoattractant and greater in *pi3k1/2/3* than in *pi3k1/2* null cells. We found that some of the *pi3k1/2/3* null cells moved perpendicular to the gradient or away from the chemoattractant source, indicating an impairment in the ability to sense the chemoattractant gradient. This phenotype was more severe at lower concentrations of chemoattractant. These observations suggest that, as the PI3K levels decrease, cells have increasing difficulty sensing the chemoattractant gradient, and these defects are more severe in weaker chemoattractant gradients. Our findings are consistent with models in which PI3K plays a part in gradient sensing but is not required or is less essential if the gradient is sufficiently steep or the concentration of chemoattractant is high. Our findings are consistent with the observations of Loovers *et al.* (16) that under some conditions *pi3k1/2* null cells move well toward the chemoattractant source and that at low chemoattractant concentrations, LY294002 can block chemotaxis (42). These observations indicate that, as proposed before, other pathways are able to mediate directional sensing (16). We suggest that PI3K plays an important part in signal amplification to mediate the localized production of F-actin (13, 29). We think this pathway plays a key role in the ability of cells to detect and rapidly respond to weak chemoattractant signals and to establish a directional response. Once cells become well polarized, PI3K may not play as essential a role in regulating directional sensing.

We found it particularly interesting that, as *pi3k1/2/3* null cells chemotax for longer periods of time, the speed of cell movement and the directionality increases. The increase in persistence is independent from a change in chemotactic speed. We cannot exclude the possibility that this change is mediated by changes in transcription or translation in response to receptor stimulation, but we suggest that the basis for this behavior is that other signaling pathways become increasingly active or amplified at the leading edge and "compensate" for the low level of PI3K signaling. We demonstrated previously that the signaling pathways become amplified at the leading edge in part through F-actin-mediated recruitment of a number of signaling components (13). We suggest that, with time, the signaling complexes required for cell movement amplify at the leading edge, and this takes longer in the absence of PI3K. We find (as was observed previously) that once LY294002-treated cells finally polarize, they can move effectively. However, this takes 15 min under our conditions and 6–10 min under the conditions used by Loovers *et al.* (16). We expect that LY294002 inhibits other members of the PI3K family in addition to Class I PI3Ks (*i.e.* TORC2 and possible others; Ref. 40), and we do not understand how these pathways intersect to inhibit or stimulate cell movement. Moreover, although RacB activation is lower in *pi3k1/2* null cells and higher in *pten* null cells, its expression shows an inverse correlation, indicating that a compensatory feedback loop also affects the parameters of signaling (30).

In conclusion, the pathways regulating the speed, polarity, and directionality of cell movement are complex, and more than one pathway is required for directional sensing. Our studies support the idea that PI3K plays a vital part in directional sensing and the initial stages of properly localizing the leading edge response relative to the chemoattractant gradient. As cells become more polarized, a process that is related to the stabilization of leading and posterior ends of the cell, other pathways are able to regulate directional movement. In weaker gradients these other pathways cannot fully compensate for a loss of PI3K, and the directionality of chemotaxis becomes weaker. Because cells lacking essentially all PI3K function can still move toward the chemoattractant gradient, there must be other signaling pathways that can mediate directional sensing, although the movement is less efficient in the absence of PI3K. We suggest that the relative importance of these pathways in directional sensing is a function of the gradient strength and shape. In weaker gradients, cells require both PI3K and a second signaling pathway, whereas either pathway may be expendable in strong gradients as the sensing ability of only one of the pathways is sufficient. PI3K also has a separate role in mediating speed, possibly through a regulation of the efficiency of F-actin polymerization.

Acknowledgments—We thank members of the Firtel laboratory for their many helpful suggestions.

REFERENCES

1. Charest, P. G., and Firtel, R. A. (2006) *Curr. Opin. Genet. Dev.* **16,** 339–347
2. Bagorda, A., Mihaylov, V. A., and Parent, C. A. (2006) *Thromb. Haemostasis* **95,** 12–21
3. Barber, M. A., and Welch, H. C. (2006) *Bull. Cancer* **93,** 44–52
4. Van Haastert, P. J., and Devreotes, P. N. (2004) *Nat. Rev. Mol. Cell Biol.* **5,** 626–634
5. Haugh, J. M., Codazzi, F., Teruel, M., and Meyer, T. (2000) *J. Cell Biol.* **151,**

1269–1280
6. Servant, G., Weiner, O. D., Herzmark, P., Balla, T., Sedat, J. W., and Bourne, H. R. (2000) *Science* **287,** 1037–1040
7. Meili, R., Ellsworth, C., Lee, S., Reddy, T. B., Ma, H., and Firtel, R. A. (1999) *EMBO J.* **18,** 2092–2105
8. Parent, C. A., Blacklock, B. J., Froehlich, W. M., Murphy, D. B., and Devreotes, P. N. (1998) *Cell* **95,** 81–91
9. Meili, R., Ellsworth, C., and Firtel, R. A. (2000) *Curr. Biol.* **10,** 708–717
10. Funamoto, S., Milan, K., Meili, R., and Firtel, R. A. (2001) *J. Cell Biol.* **153,** 795–809
11. Comer, F. I., Lippincott, C. K., Masbad, J. J., and Parent, C. A. (2005) *Curr. Biol.* **15,** 134–139
12. Funamoto, S., Meili, R., Lee, S., Parry, L., and Firtel, R. A. (2002) *Cell* **109,** 611–623
13. Sasaki, A. T., Chun, C., Takeda, K., and Firtel, R. A. (2004) *J. Cell Biol.* **167,** 505–518
14. Wang, F., Herzmark, P., Weiner, O. D., Srinivasan, S., Servant, G., and Bourne, H. R. (2002) *Nat. Cell Biol.* **4,** 513–518
15. Sasaki, A. T., and Firtel, R. A. (2006) *Eur. J. Cell Biol.* **85,** 873–895
16. Loovers, H. M., Postma, M., Keizer-Gunnink, I., Huang, Y. E., Devreotes, P. N., and van Haastert, P. J. (2006) *Mol. Biol. Cell* **17,** 1503–1513
17. Hirsch, E., Katanaev, V., Garlanda, C., Azzolino, O., Pirola, L., Silengo, L., Sozzani, S., Mantovani, A., Altruda, F., and Wymann, M. (2000) *Science* **287,** 1049–1053
18. Li, Z., Jiang, H., Xie, W., Zhang, Z., Smrcka, A., and Wu, D. (2000) *Science* **287,** 1046–1049
19. Van Keymeulen, A., Wong, K., Knight, Z. A., Govaerts, C., Hahn, K. M., Shokat, K. M., and Bourne, H. R. (2006) *J. Cell Biol.* **174,** 437–445
20. Vanhaesebroeck, B., Jones, G. E., Allen, W. E., Zicha, D., Hooshmand-Rad, R., Sawyer, C., Wells, C., Waterfield, M. D., and Ridley, A. J. (1999) *Nat. Cell Biol.* **1,** 69–71
21. Chung, C. Y., Funamoto, S., and Firtel, R. A. (2001) *Trends Biochem. Sci.* **26,** 557–566
22. Bourne, H. R. (2005) *Nat. Cell Biol.* **7,** 777–778
23. Kunisaki, Y., Nishikimi, A., Tanaka, Y., Takii, R., Noda, M., Inayoshi, A., Watanabe, K., Sanematsu, F., Sasazuki, T., Sasaki, T., and Fukui, Y. (2006) *J. Cell Biol.* **174,** 647–652
24. Nombela-Arrieta, C., Lacalle, R. A., Montoya, M. C., Kunisaki, Y., Megias, D., Marques, M., Carrera, A. C., Manes, S., Fukui, Y., Martinez, A. C., and Stein, J. V. (2004) *Immunity* **21,** 429–441
25. Reif, K., and Cyster, J. (2002) *Trends Cell Biol.* **12,** 368–373
26. Cote, J. F., Motoyama, A. B., Bush, J. A., and Vuori, K. (2005) *Nat. Cell Biol.* **7,** 797–807
27. Mouneimne, G., Soon, L., DesMarais, V., Sidani, M., Song, X., Yip, S. C., Ghosh, M., Eddy, R., Backer, J. M., and Condeelis, J. (2004) *J. Cell Biol.* **166,** 697–708
28. Hill, K., Welti, S., Yu, J., Murray, J. T., Yip, S. C., Condeelis, J. S., Segall, J. E., and Backer, J. M. (2000) *J. Biol. Chem.* **275,** 3741–3744
29. Chen, L., Janetopoulos, C., Huang, Y. E., Iijima, M., Borleis, J., and Devreotes, P. N. (2003) *Mol. Biol. Cell* **14,** 5028–5037
30. Park, K. C., Rivero, F., Meili, R., Lee, S., Apone, F., and Firtel, R. A. (2004) *EMBO J.* **23,** 4177–4189
31. Janetopoulos, C., Borleis, J., Vazquez, F., Iijima, M., and Devreotes, P. (2005) *Dev. Cell* **8,** 467–477
32. Wessels, D., Voss, E., Von Bergen, N., Burns, R., Stites, J., and Soll, D. R. (1998) *Cell. Motil. Cytoskel.* **41,** 225–246
33. Kimmel, A. R., and Parent, C. A. (2003) *Science* **300,** 1525–1527
34. Aubry, L., and Firtel, R. (1999) *Annu. Rev. Cell Dev. Biol.* **15,** 469–517
35. Insall, R. H., Soede, R. D., Schaap, P., and Devreotes, P. N. (1994) *Mol. Biol. Cell* **5,** 703–711
36. Kriebel, P. W., Barr, V. A., and Parent, C. A. (2003) *Cell* **112,** 549–560
37. Devreotes, P., and Janetopoulos, C. (2003) *J. Biol. Chem.* **278,** 20445–20448
38. Comer, F. I., and Parent, C. A. (2006) *Mol. Biol. Cell* **17,** 357–366
39. Zhou, K., Takegawa, K., Emr, S. D., and Firtel, R. A. (1995) *Mol. Cell. Biol.* **15,** 5645–5656
40. Lee, S., Comer, F. I., Sasaki, A., McLeod, I. X., Duong, Y., Okumura, K., Yates, J. R., III, Parent, C. A., and Firtel, R. A. (2005) *Mol. Biol. Cell* **16,** 4572–4583
41. Iijima, M., and Devreotes, P. (2002) *Cell* **109,** 599–610
42. Postma, M., Roelofs, J., Goedhart, J., Loovers, H. M., Visser, A. J., and Van Haastert, P. J. (2004) *J. Cell Sci.* **117,** 2925–2935